Composite Structures 101 (2013) 94–103

Contents lists available at SciVerse ScienceDirect

Composite Structures

journal homepage: www.elsevier.com/locate/compstruct

Static and dynamic analysis of thick laminated plates using enriched macroelements

Rita F. Rango [a,*], Liz G. Nallim [a,b], Sergio Oller [b]

[a] Facultad de Ingeniería, INIQUI (CONICET), Universidad Nacional de Salta, Av. Bolivia 5150, 4400 Salta, Argentina
[b] International Center for Numerical Methods in Engineering (CIMNE), Universitat Politècnica de Catalunya, Edif. C1, Campus Nord, Jordi Girona 1-3, 08034 Barcelona, Spain

ARTICLE INFO

Article history:
Available online 9 February 2013

Keywords:
Thick laminated plates
Macroelement
First-order shear deformation theory

ABSTRACT

The development, computational implementation and application of polynomially-enriched plate macroelement are presented in this work. This macro-element has been formulated by the authors for thin isotropic plates using Gram–Schmidt orthogonal polynomials as enrichment functions and, in this work, the first-order shear deformation theory and the material anisotropy is incorporated. For taking into account plates of several geometrical shapes, an arbitrary quadrilateral laminate is mapped onto a square basic one, so that a unique macro-element can be constructed. The obtained formulation is applied to the static and dynamic analysis of thick composite laminated plates. Besides, it is possible to study generally coplanar plate assemblies by combining two or more macro-elements via a special connectivity matrix. Thus, hierarchically enriched global stiffness matrix, mass matrix, and loading vector of general laminated plate structure are derived. Several different boundary conditions may be arranged in the analysis. This procedure gives a matrix equation of static equilibrium and a matrix-eigenvalue problem that can be solved with optimum efficiency. Numerical obtained results show very good correlation with published results. Besides, the formulation produces stable results and it is computationally efficient.

1. Introduction

Composite structures, specially laminated composite plates, are increasingly used in many engineering fields such as civil, marine and aerospace structures, because of their high strength and stiffness to weight ratios. Laminated composite plates allow the controllability of the structural properties through changing the fibre orientation angles, the number of plies and selecting proper composite materials. With the wide use of composite structures in modern industries, mechanical analysis of plates of complex geometry becomes a relevant topic. The solutions to the plate problems are strongly dependent on the geometrical shapes, boundary conditions and material properties. It is widely recognized that closed form solutions are possible only for a few specific cases. The determination of classical solutions (exact and/or approximate) which correspond to the static and dynamic behaviour of anisotropic plates of different shapes and configurations has been studied and is well documented. The bending of anisotropic plates subjected to different normal loads and boundary conditions has been extensively studied (see, for instance, Refs. [1–3]). There are several complete reviews on static behaviour of composite and sandwich plates. Moleiro et al. [4] and Auricchio et al. [5] presented static analysis of square plates using a mixed first-order shear deformation theory into a finite element model. Wang et al. [6] analyzed the static and dynamic behaviour of rectangular plates via FSDT meshless method. Other authors also developed different alternative solutions for rectangular anisotropic plates employing the first order and a refined zigzag theory [7], or various shear deformation theories together with meshless methods [8]. Ferreira et al. [9] presented static and vibration analysis of laminated composite plates using FSDT based on a high order collocation method. The available literature shows that, comparatively, most studies for static and dynamic analysis of laminated plates are mainly concerned with rectangular ones. However, plates of general shape are common industrial elements in many engineering fields like air craft wings, ship substructures, bridge entrance and vehicle bodies. Nevertheless, studies on general quadrilateral plates or polygonal plates with unequal side lengths are rather limited. For these reasons, this work presents a polynomially-enriched plate macro-element and its application to the static and free vibration analysis of moderately thick composite laminated plates of several geometries. The enriched finite macro-element is obtained using Gram–Schmidt orthogonal polynomials, while the different geometrical shapes are represented by the mapping of a square laminated plate defined in terms of its natural coordinates. The formulation presented in this work allows investigating the static and dynamic behaviour of several composite laminated plates with any combination of boundary conditions. Furthermore,

* Corresponding author. Tel.: +54 3874255336.
E-mail addresses: ritarango@conicet.gov.ar (R.F. Rango), sergio.oller@upc.edu (S. Oller).
URLs: http://www.unsa.edu.ar, http://www.conicet.gob.ar (R.F. Rango), http://www.upc.edu, http://www.cimne.com (S. Oller).

0263-8223/$ - see front matter © 2013 Elsevier Ltd. All rights reserved.
http://dx.doi.org/10.1016/j.compstruct.2013.01.028

the described assembly process enables to encompass plates of more complex geometry. Finally, to demonstrate the validity and efficiency of the proposed method, numerical examples are solved and some of them are verified with results from others authors.

2. Mathematical formulation

Let us consider a thick laminated composite plate with an arbitrary-shaped quadrilateral planform as shown in Fig. 1. The laminate is of uniform thickness h and is made up of a number of layers each consisting of unidirectional fibre reinforced composite material. The fibre angle of the kth layer counted from the surface $z = -h/2$ is β, measured from the x axis to the fibre orientation, with all laminate having equal thicknesses. Symmetric lamination of plies is considered in this work.

Based on the First-order Shear Deformation Theory (FSDT) [10,11] the displacement field of a laminated composite plate is expressed as:

$$\begin{aligned} u(x,y,z) &= z\phi_x(x,y) \\ v(x,y,z) &= z\phi_y(x,y) \\ w(x,y,z) &= w_0(x,y) \end{aligned} \tag{1}$$

where (u,v,w) are the displacements of a generic point (x,y,z) in the laminate, w_0 is the displacement of a corresponding point on the mid-plane, and (ϕ_x,ϕ_y) denote the rotations of the transverse normal about y and x axis, respectively.

2.1. Transformation of coordinates

Some authors have used the mapping technique, as commonly employed in finite element analysis, in conjunction with other methods to study the mechanical behaviour of plates of various geometrical shapes. Nallim et al. [12] combined the mapping technique and the Ritz method to derive a general formulation for the analysis of symmetrically laminated plates. Also, Nallim and Oller [13] extended that previous work together with the mapping technique to the general case of unsymmetrically laminated plates. Applying the same concept, an arbitrarily shaped quadrilateral plate in Cartesian coordinates, may be expressed simply by mapping a parent square plate, which will be called master plate, defined in the natural coordinates by the simple boundary equations $\xi = \pm 1$ and $\eta = \pm 1$ (Fig. 2).

The mapping of the Cartesian coordinate system is given by [14,15]:

$$\begin{aligned} x &= \sum_{i=1}^{4} N_i(\xi,\eta)x_i \\ y &= \sum_{i=1}^{4} N_i(\xi,\eta)y_i \end{aligned} \tag{2}$$

where (x_i,y_i), $i = 1,\ldots,4$ are the coordinates of the four corners of the quadrilateral region R and $N_i(\xi,\eta)$ are the interpolation functions of the serendipity family given by:

$$N_i(\xi,\eta) = \frac{1}{4}(1+\eta_i\eta)(1+\xi_i\xi) \tag{3}$$

The transformation (2) maps a point (ξ,η) in the master plate $\overline{R}$ onto a point (x,y) in the real plate domain R and vice versa if the Jacobian determinant of the transformation given by:

$$|\mathbf{J}| = \frac{\partial x}{\partial \xi}\frac{\partial y}{\partial \eta} - \frac{\partial x}{\partial \eta}\frac{\partial y}{\partial \xi} \tag{4}$$

is positive.

Applying the chain rule of differentiation it can be shown that the first derivatives of a function in both spaces are related by:

$$\begin{bmatrix} \frac{\partial}{\partial x} \\ \frac{\partial}{\partial y} \end{bmatrix} = \mathbf{J}^{-1}\begin{bmatrix} \frac{\partial}{\partial \xi} \\ \frac{\partial}{\partial \eta} \end{bmatrix} = \begin{bmatrix} \frac{J_{22}}{|\mathbf{J}|} & -\frac{J_{12}}{|\mathbf{J}|} \\ -\frac{J_{21}}{|\mathbf{J}|} & \frac{J_{11}}{|\mathbf{J}|} \end{bmatrix}\begin{bmatrix} \frac{\partial}{\partial \xi} \\ \frac{\partial}{\partial \eta} \end{bmatrix} \tag{5}$$

where $\mathbf{J}$ is the Jacobian given by:

$$\mathbf{J} = \begin{bmatrix} J_{11} & J_{12} \\ J_{21} & J_{22} \end{bmatrix} = \begin{bmatrix} \sum x_i N_{i,\xi} & \sum y_i N_{i,\xi} \\ \sum x_i N_{i,\eta} & \sum y_i N_{i,\eta} \end{bmatrix} \tag{6}$$

The elemental area $dxdy$ in the Cartesian domain R is transformed into $|\mathbf{J}|d\xi d\eta$.

2.2. Approximating functions

The use of Gram–Schmidt orthogonal polynomials to study anisotropic plates is very satisfactory, as has been demonstrated by Nallim et al. [12,13,16], since the convergence of the solution is rapid and practically without oscillations. For this reason, in the present paper the transverse deflection and the rotations are expressed in terms of the natural coordinates system by sets of polynomials $\{p_i(\xi)\}$ and $\{q_j(\eta)\}$, of which the first two polynomials are Hermite polynomials and then an adequate number of Gram–Schmidt polynomials are added to formulate a polynomially-enriched plate macro-element. This macro-element has been formulated by the authors for thin plates [17].

Then, the components of displacement field can be expressed as:

$$\begin{aligned} w(\xi,\eta) &= \sum_{i,j=1}^{n} c_{ij}^{w} p_i(\xi)q_j(\eta) \\ \phi_x(\xi,\eta) &= \sum_{i,j=1}^{n} c_{ij}^{\phi x} p_i(\xi)q_j(\eta) \\ \phi_y(\xi,\eta) &= \sum_{i,j=1}^{n} c_{ij}^{\phi y} p_i(\xi)q_j(\eta) \end{aligned} \tag{7}$$

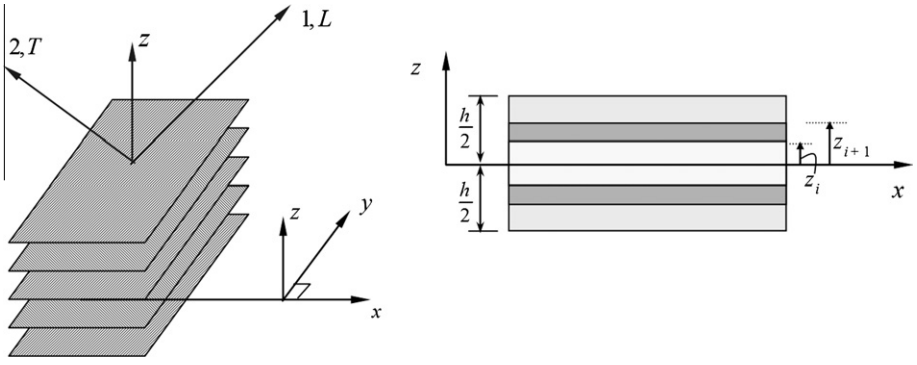

Fig. 1. Geometry of an N-layered symmetric laminate.

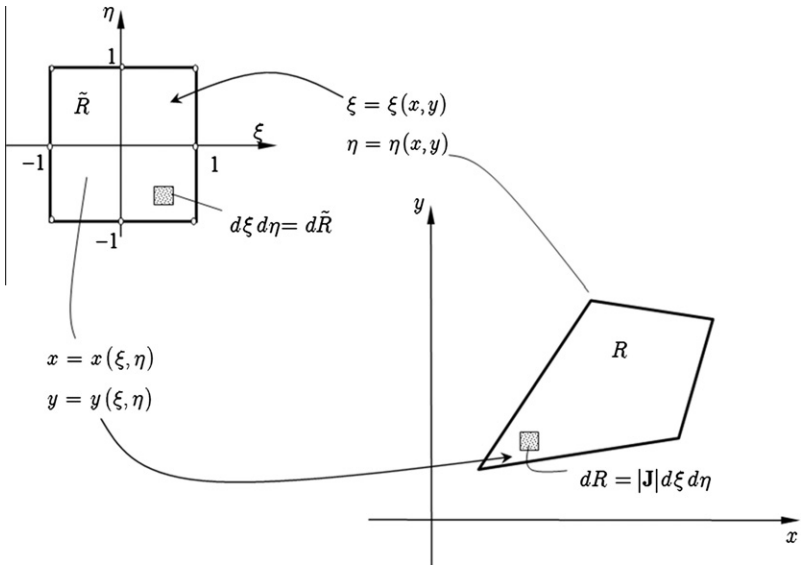

Fig. 2. Mapping of an arbitrary quadrilateral plate into natural coordinates.

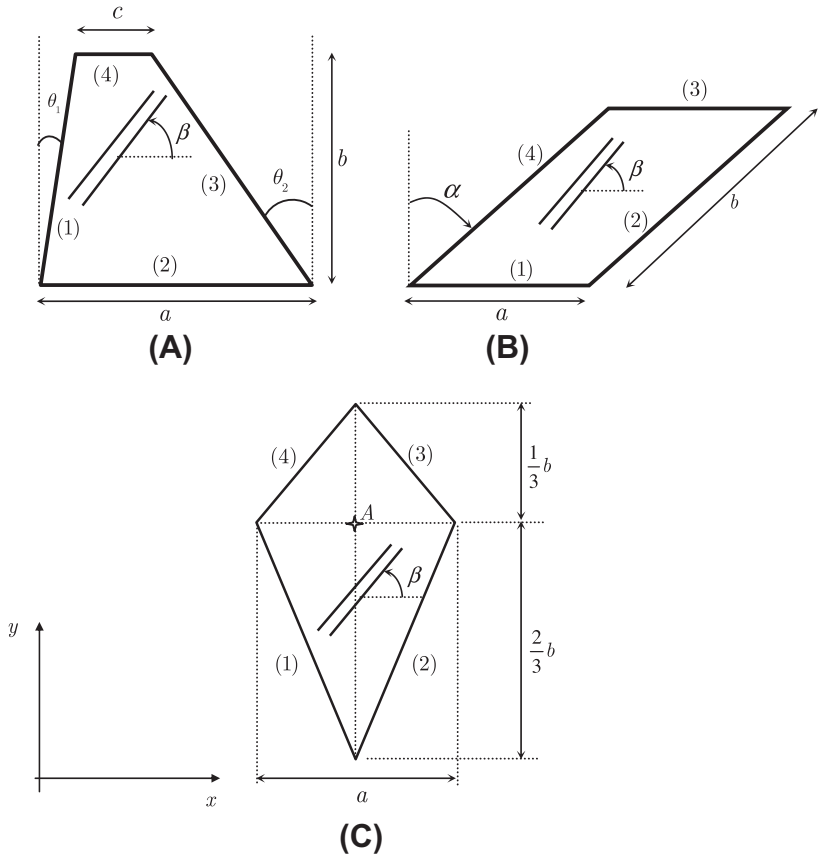

Fig. 3. Laminates of various shapes.

where c_{ij}^{w}, $c_{ij}^{\phi x}$ and $c_{ij}^{\phi y}$ are the unknown coefficients, $p_1(\xi)$ and $p_2(\xi)$ are Hermite polynomials in the ξ direction given by:

$$p_1(\xi) = -\frac{1}{2}\xi + \frac{1}{2}, \quad p_2(\xi) = \frac{1}{2}\xi + \frac{1}{2} \tag{8}$$

The Gram–Schmidt polynomial in the ξ direction is as follows:

$$p_3(\xi) = -1 + \xi^2 \tag{9}$$

This polynomial satisfies the condition $p_3(\xi)|_{\xi=-1} = p_3(\xi)|_{\xi=1} = 0$ in order to contribute only to the internal displacement field of the element.

The higher members of the set $\{p_i(\xi)\}$, $i = 4, \ldots, n$ are constructed by employing the Gram–Schmidt orthogonalization procedure, as has been proposed by Bhat [18,19]. The coefficients of the polynomials are chosen in such a way as to make the polynomials orthonormal, $\int_{-1}^{1} p_k^2(\xi) = 1$.

The polynomials along the η direction are also generated using the same procedure. It is important to point out that working with the master element in natural coordinates allows us to use the same set of orthogonal polynomials for plates of different geometric shapes. This fact makes possible a unified treatment.

The Hermite polynomials confer displacement or rotations to each corner of the element. These are recognized as the linear displacement functions used in the standard h-version of the Finite Element Method (FEM) [14,15]. The subsequent assumed polynomials, the Gram–Schmidt polynomials, have zero displacement at each end. These hierarchical polynomials contribute only to the internal displacement field of the element, and do not therefore affect the displacement and rotations along the element edge. However, when any of these hierarchical polynomials are used in conjunction with the Hermite ones, they will constitute what amounts to an edge degree of freedom along the element boundaries. Adjacent elements may be joined by ensuring compatibility of both nodal and edge displacements; this procedure guarantees that all element-to-element interfaces are fully conforming, as has been demonstrated by Bardell et al. [20].

3. Governing equations

3.1. Stiffness matrix

For the selected problems, let us consider a symmetric laminate of total uniform thickness h, composed of a number of orthotropic layers. Considering the established kinematics and basic assumptions of the first order theory, the strain energy is given by:

$$\begin{aligned}U=\frac{1}{2}\int\int_R (&k_sA_{44}\left(\phi_y+\frac{\partial w}{\partial y}\right)^2\\&+2k_sA_{45}\left(\phi_x+\frac{\partial w}{\partial x}\right)\left(\frac{\partial w}{\partial y}+\phi_y\right)+k_sA_{55}\left(\phi_x+\frac{\partial w}{\partial x}\right)^2\\&+D_{11}\left(\frac{\partial\phi_x}{\partial x}\right)^2+2D_{12}\frac{\partial\phi_x}{\partial x}\frac{\partial\phi_y}{\partial y}+D_{22}\left(\frac{\partial\phi_y}{\partial y}\right)^2+2D_{16}\\&\times\frac{\partial\phi_x}{\partial x}\left(\frac{\partial\phi_x}{\partial y}+\frac{\partial\phi_y}{\partial x}\right)+2D_{26}\frac{\partial\phi_y}{\partial y}\left(\frac{\partial\phi_x}{\partial y}+\frac{\partial\phi_y}{\partial x}\right)\\&+D_{66}\left(\frac{\partial\phi_x}{\partial y}+\frac{\partial\phi_y}{\partial x}\right)^2)dxdy\end{aligned}\tag{10}$$

where R is the mid-surface area and k_s is the shear correction factor.

In Eq. (10) the bending stiffness and transverse shearing stiffness are respectively given by:

$$\begin{aligned}D_{ij}&=\int_{-h/2}^{h/2}z^2\overline{Q}_{ij}dz\quad i,\ j=1,2,6\\A_{ij}&=\int_{-h/2}^{h/2}\overline{Q}_{ij}dz\quad i,\ j=4,5\end{aligned}\tag{11}$$

where $\overline{Q}_{ij}$ are the mechanical reduced rigidities referred to x, y axes [1,3].

The strain energy given by Eq. (10) can be rewritten as:

$$\begin{aligned}U=&\frac{1}{2}\int\int_R k_s\left[\left(\phi_y+\frac{\partial w}{\partial y}\right)\left(\phi_x+\frac{\partial w}{\partial x}\right)\right]\begin{bmatrix}A_{44}&A_{45}\\A_{45}&A_{55}\end{bmatrix}\begin{bmatrix}\left(\phi_y+\frac{\partial w}{\partial y}\right)\\\left(\phi_x+\frac{\partial w}{\partial x}\right)\end{bmatrix}dxdy\\&+\frac{1}{2}\int\int_R\begin{bmatrix}\frac{\partial\phi_x}{\partial x}&\frac{\partial\phi_y}{\partial y}&\frac{\partial\phi_x}{\partial y}+\frac{\partial\phi_y}{\partial x}\end{bmatrix}\begin{bmatrix}D_{11}&D_{12}&D_{16}\\D_{12}&D_{22}&D_{26}\\D_{16}&D_{26}&D_{66}\end{bmatrix}\begin{bmatrix}\frac{\partial\phi_x}{\partial x}\\\frac{\partial\phi_y}{\partial y}\\\frac{\partial\phi_x}{\partial y}+\frac{\partial\phi_y}{\partial x}\end{bmatrix}dxdy\end{aligned}\tag{12}$$

By substituting Eq. (7) into Eq. (12), we can obtain the following equation:

$$\begin{aligned}U=&\frac{1}{2}\int_{-1}^{1}\int_{-1}^{1}k_s\left[\left(\{N_f\}\{c^{\phi y}\}+\left\{\frac{\partial N_f}{\partial y}\right\}\{c^w\}\right),\right.\\&\left.\left(\{N_f\}\{c^{\phi x}\}+\left\{\frac{\partial N_f}{\partial x}\right\}\{c^w\}\right)\right]\begin{bmatrix}A_{44}&A_{45}\\A_{45}&A_{55}\end{bmatrix}\\&\times\begin{bmatrix}\left(\{N_f\}\{c^{\phi y}\}+\left\{\frac{\partial N_f}{\partial y}\right\}\{c^w\}\right)\\\left(\{N_f\}\{c^{\phi x}\}+\left\{\frac{\partial N_f}{\partial x}\right\}\{c^w\}\right)\end{bmatrix}|\mathbf{J}|d\xi d\eta\\&+\frac{1}{2}\int_{-1}^{1}\int_{-1}^{1}\left[\left\{\frac{\partial N_f}{\partial x}\right\}\{c^{\phi x}\},\left\{\frac{\partial N_f}{\partial y}\right\}\{c^{\phi y}\},\right.\\&\left.\left(\left\{\frac{\partial N_f}{\partial y}\right\}\{c^{\phi x}\}+\left\{\frac{\partial N_f}{\partial x}\right\}\{c^{\phi y}\}\right)\right]\begin{bmatrix}D_{11}&D_{12}&D_{16}\\D_{12}&D_{22}&D_{26}\\D_{16}&D_{26}&D_{66}\end{bmatrix}\\&\times\begin{bmatrix}\left\{\frac{\partial N_f}{\partial x}\right\}\{c^{\phi x}\}\\\left\{\frac{\partial N_f}{\partial y}\right\}\{c^{\phi y}\}\\\left(\left\{\frac{\partial N_f}{\partial y}\right\}\{c^{\phi x}\}+\left\{\frac{\partial N_f}{\partial x}\right\}\{c^{\phi y}\}\right)\end{bmatrix}|\mathbf{J}|d\xi d\eta\end{aligned}\tag{13}$$

where

$$\begin{aligned}&N_f=N_f(\xi,\eta)=[p_i(\xi)q_j(\eta)]\ i,j=1\ldots n\\&[N_f]=[p_1q_1\ \ p_1q_2\ \ p_1q_3\ \ p_1q_4\ \ p_1q_5\ \ \cdots\ \ p_1q_n\ \ p_2q_1\ \ p_2q_2\ \ p_2q_3\ \ \cdots\ \ p_nq_n]\end{aligned}\tag{14}$$

and the unknown coefficients are:

$$\begin{aligned}[c^w]&=[c^w_{11}\ \ c^w_{12}\ \ c^w_{13}\ \ c^w_{14}\ \ c^{15}_w\ \ \ldots\ \ c^{1n}_w\ \ c^{21}_w\ \ c^{22}_w\ \ c^{23}_w\ldots\ \ c^{\mathrm{nn}}_w]^T\\[c^{\phi x}]&=[c^{\phi x}_{11}\ \ c^{\phi x}_{12}\ \ c^{\phi x}_{13}\ \ c^{\phi x}_{14}\ \ c^{\phi x}_{15}\ \ \ldots\ \ c^{\phi x}_{1n}\ \ c^{\phi x}_{21}\ \ c^{\phi x}_{22}\ \ c^{\phi x}_{23}\ \ \ldots\ \ c^{\phi x}_{nn}]^T\\[c^{\phi y}]&=[c^{\phi y}_{11}\ \ c^{\phi y}_{12}\ \ c^{\phi y}_{13}\ \ c^{\phi y}_{14}\ \ c^{\phi y}_{15}\ \ \ldots\ \ c^{\phi y}_{1n}\ \ c^{\phi y}_{21}\ \ c^{\phi y}_{22}\ \ c^{\phi y}_{23}\ \ \ldots\ \ c^{\phi y}_{nn}]^T\end{aligned}\tag{15}$$

Finally, taking into account Eqs. (14) and (15) the strain energy results:

$$\begin{aligned}U=&\frac{1}{2}\int_{-1}^{1}\int_{-1}^{1}k_s\begin{bmatrix}\mathbf{c}^w&\mathbf{c}^{\phi x}&\mathbf{c}^{\phi y}\end{bmatrix}\begin{bmatrix}\frac{\partial\mathbf{N}_f}{\partial y}&\frac{\partial\mathbf{N}_f}{\partial x}\\\mathbf{0}&\mathbf{N}_f\\\mathbf{N}_f&\mathbf{0}\end{bmatrix}\begin{bmatrix}A_{44}&A_{45}\\A_{45}&A_{55}\end{bmatrix}\begin{bmatrix}\frac{\partial\mathbf{N}_f}{\partial y}&\mathbf{0}&\mathbf{N}_f\\\frac{\partial\mathbf{N}_f}{\partial x}&\mathbf{N}_f&\mathbf{0}\end{bmatrix}\\&\times\begin{bmatrix}\mathbf{c}^w\\\mathbf{c}^{\phi x}\\\mathbf{c}^{\phi y}\end{bmatrix}|\mathbf{J}|d\xi d\eta+\frac{1}{2}\int_{-1}^{1}\int_{-1}^{1}\begin{bmatrix}\mathbf{c}^w&\mathbf{c}^{\phi x}&\mathbf{c}^{\phi y}\end{bmatrix}\begin{bmatrix}\mathbf{0}&\mathbf{0}&\mathbf{0}\\\frac{\partial\mathbf{N}_f}{\partial x}&\mathbf{0}&\frac{\partial\mathbf{N}_f}{\partial y}\\\mathbf{0}&\frac{\partial\mathbf{N}_f}{\partial y}&\frac{\partial\mathbf{N}_f}{\partial x}\end{bmatrix}\\&\times\begin{bmatrix}D_{11}&D_{12}&D_{16}\\D_{12}&D_{22}&D_{26}\\D_{16}&D_{26}&D_{66}\end{bmatrix}\begin{bmatrix}\mathbf{0}&\frac{\partial\mathbf{N}_f}{\partial x}&\mathbf{0}\\\mathbf{0}&\mathbf{0}&\frac{\partial\mathbf{N}_f}{\partial y}\\\mathbf{0}&\frac{\partial\mathbf{N}_f}{\partial y}&\frac{\partial\mathbf{N}_f}{\partial x}\end{bmatrix}\begin{bmatrix}\mathbf{c}^w\\\mathbf{c}^{\phi x}\\\mathbf{c}^{\phi y}\end{bmatrix}|\mathbf{J}|d\xi d\eta\end{aligned}\tag{16}$$

The macro-element stiffness matrix can be written, based on the Hamilton's principle, as:

$$\begin{aligned}[K]=&\int_{-1}^{1}\int_{-1}^{1}k_s\begin{bmatrix}\frac{\partial\mathbf{N}_f}{\partial y}&\frac{\partial\mathbf{N}_f}{\partial x}\\\mathbf{0}&\mathbf{N}_f\\\mathbf{N}_f&\mathbf{0}\end{bmatrix}\begin{bmatrix}A_{44}&A_{45}\\A_{45}&A_{55}\end{bmatrix}\begin{bmatrix}\frac{\partial\mathbf{N}_f}{\partial y}&\mathbf{0}&\mathbf{N}_f\\\frac{\partial\mathbf{N}_f}{\partial x}&\mathbf{N}_f&\mathbf{0}\end{bmatrix}|\mathbf{J}|d\xi d\eta\\&+\int_{-1}^{1}\int_{-1}^{1}\begin{bmatrix}\mathbf{0}&\mathbf{0}&\mathbf{0}\\\frac{\partial\mathbf{N}_f}{\partial x}&\mathbf{0}&\frac{\partial\mathbf{N}_f}{\partial y}\\\mathbf{0}&\frac{\partial\mathbf{N}_f}{\partial y}&\frac{\partial\mathbf{N}_f}{\partial x}\end{bmatrix}\begin{bmatrix}D_{11}&D_{12}&D_{16}\\D_{12}&D_{22}&D_{26}\\D_{16}&D_{26}&D_{66}\end{bmatrix}\begin{bmatrix}\mathbf{0}&\frac{\partial\mathbf{N}_f}{\partial x}&\mathbf{0}\\\mathbf{0}&\mathbf{0}&\frac{\partial\mathbf{N}_f}{\partial y}\\\mathbf{0}&\frac{\partial\mathbf{N}_f}{\partial y}&\frac{\partial\mathbf{N}_f}{\partial x}\end{bmatrix}|\mathbf{J}|d\xi d\eta\end{aligned}\tag{17}$$

3.2. External forces

The potential energy of a transversal load $q_0(x,y)$ distributed over the plate surface (R) is given by:

$$V = -\int\int_R q_0(x,y) w \, dx \, dy \tag{18}$$

By substituting Eq. (7) into Eq. (18), and considering the Hamilton's principle we can obtain the external forces vector as:

$$\{F\} = -q_0 \int_{-1}^{1}\int_{-1}^{1} [N_f]^T |\mathbf{J}| d\xi \, d\eta \tag{19}$$

3.3. Mass matrix

The kinetic energy for free vibrations of the plate is given by:

$$T = \frac{1}{2}\int\int_V\int \rho\left[\left(\frac{\partial u}{\partial t}\right)^2 + \left(\frac{\partial v}{\partial t}\right)^2 + \left(\frac{\partial w}{\partial t}\right)^2\right] dx\,dy\,dz \tag{20}$$

where ρ is the material density, which is considered here to be uniform through the volume of the laminate (V).

The displacement functions are assumed periodic in time, so the maximum kinetic energy in a vibratory cycle is:

$$T = \frac{1}{2}\int\int_R \rho\omega^2\left[hw^2 + \frac{h^3}{12}\phi_x^2 + \frac{h^3}{12}\phi_y^2\right] dx\,dy \tag{21}$$

where ω is the radian natural frequency.

By substituting Eq. (7) into Eq. (21), and taking into account the Hamilton's principle we can obtain the mass matrix as:

$$[M] = \int_{-1}^{1}\int_{-1}^{1} \rho h \begin{bmatrix} \mathbf{N}_f^T\mathbf{N}_f & \mathbf{0} & \mathbf{0} \\ \mathbf{0} & \frac{h^2}{12}\mathbf{N}_f^T\mathbf{N}_f & \mathbf{0} \\ \mathbf{0} & \mathbf{0} & \frac{h^2}{12}\mathbf{N}_f^T\mathbf{N}_f \end{bmatrix} |\mathbf{J}| d\xi \, d\eta \tag{22}$$

3.4. Static and free vibration problems

In order to model irregular planforms, it is now necessary to consider how to combine individual elements. The first stage in formulating an assembly process is to separate out the degrees of freedom $\{c_{ij}^w, c_{ij}^{\phi x}, c_{ij}^{\phi y}\}$ into nodal (corner), edge and purely internal degrees of freedom, and then rearrange the corresponding entries in the element stiffness and mass matrices (and load vector). Then, it is possible to form the global stiffness $[K^G]$ and mass $[M^G]$ matrices and the global load vector $\{F^G\}$ by identifying and then adding

Table 1
Convergence study for SFSF, (90/0/90/0/90), square laminated plate $\left(\bar{w} = w_0\frac{E_2h^3}{a^4q_0}100\right)$.

h/a	Source	$\bar{w}$
0.01	Present $n = 3$	2.0768
	Present $n = 4$	2.0875
	Present $n = 5$	2.5957
	Present $n = 6$	2.5957
	Moleiro et al. [4]	2.5957
0.05	Present $n = 3$	2.1893
	Present $n = 4$	2.3539
	Present $n = 5$	2.7082
	Present $n = 6$	2.7082
	Moleiro et al. [4]	2.7082
0.10	Present $n = 3$	2.5410
	Present $n = 4$	2.8415
	Present $n = 5$	3.0599
	Present $n = 6$	3.0600
	Moleiro et al. [4]	3.0600

Table 2
Centroidal deflection for SSSS, (0/90/0) square laminated plate $\left(\bar{w} = w_0\frac{E_2h^3}{a^4q_0}100\right)$.

h/a	Source	$\bar{w}$
0.05	Present	0.7712
	Reddy [1]	0.7572
	Belinha and Dinis [23]	0.7583
	Xiao et al. ($K = 1$) [24]	0.7256
0.10	Present	1.0418
	Reddy [1]	1.0219
	Belinha and Dinis [23]	1.0225
	Xiao et al. ($K = 1$) [24]	0.9465
0.20	Present	2.0357
	Reddy [1]	–
	Belinha and Dinis [23]	–
	Xiao et al. ($K = 1$) [24]	1.7572

Table 3
Centroidal deflection for SSSS, (0/90/0) skew laminated plate $\left(\bar{w} = w_0\frac{E_2h^3}{a^4q_0}100\right)$.

h/a	Source	$\bar{w}$
0.10	Present	0.8619
	Chakrabarti and Sheikh FSDT [25]	0.9182
	Chakrabarti and Sheikh RHSDT [25]	0.8814
0.20	Present	1.6527
	Chakrabarti and Sheikh FSDT [25]	1.8642
	Chakrabarti and Sheikh RHSDT [25]	1.6811

Table 4
Convergence study for SFSF right trapezoidal with $a = 1$, $b = 0.5$ and $h = 0.1b\left(\bar{\omega} = \frac{\omega b^2}{h}\sqrt{\frac{\rho}{E_2}}\right)$.

Source	$\bar{w}_1$	$\bar{w}_2$	$\bar{w}_3$
(0/90/90/0)			
Present $n = 3$	5.7779	13.3079	23.6391
Present $n = 4$	5.4254	11.9664	17.6758
Present $n = 5$	5.2728	11.2116	16.2064
Present $n = 6$	5.2607	11.1408	15.4678
Zamani et al. [26]	5.4563	11.2542	16.0392
(30/60/60/30)			
Present $n = 3$	5.5002	15.6608	25.4215
Present $n = 4$	4.6272	10.2732	13.5640
Present $n = 5$	4.1196	9.2204	11.1098
Present $n = 6$	4.0406	8.7365	9.9018
Zamani et al. [26]	4.1514	8.6176	9.8155

Table 5
Dimensionless frequencies for (0/90/0) square laminated plate $\left(\bar{\omega} = \frac{\omega b^2}{\pi^2}\sqrt{\frac{\rho h}{D_0}}\right)$.

h/a	Source	$\bar{w}_1$	$\bar{w}_2$	$\bar{w}_3$
SSSS				
0.001	Present	6.6270	9.4665	16.3962
	Ferreira and Fasshauer [27]	6.6226	9.5306	16.4255
0.050	Present	6.1289	8.8774	15.0919
	Ferreira and Fasshauer [27]	6.1365	8.8846	15.1061
0.100	Present	5.1457	7.7242	12.9065
	Ferreira and Fasshauer [27]	5.1652	7.7549	12.9129
0.150	Present	4.2484	6.6337	9.4672
	Ferreira and Fasshauer [27]	4.2741	6.6657	9.4875
0.200	Present	3.5649	5.7417	7.3647
	Ferreira and Fasshauer [27]	3.5934	5.7683	7.3968
CCCC				
0.001	Present	14.7086	17.7335	26.9921
	Ferreira and Fasshauer [27]	14.6918	18.4741	26.9611
0.050	Present	10.9578	14.1253	20.3958
	Ferreira and Fasshauer [27]	10.9530	14.0235	20.3851
0.100	Present	7.4127	10.4611	13.9342
	Ferreira and Fasshauer [27]	7.4107	10.3930	13.9124
0.150	Present	5.5492	8.1867	9.9126
	Ferreira and Fasshauer [27]	5.5481	8.1467	9.9039
0.200	Present	4.4472	6.6654	7.7043
	Ferreira and Fasshauer [27]	4.4465	6.6420	7.6995

Table 6
Dimensionless frequencies for right trapezoidal with $a = 1$, $b = 0.5$ and $h = 0.1b$, $\left(\bar{\omega} = \frac{\omega b^2}{h}\sqrt{\frac{\rho}{E_2}}\right)$.

B.C.	Lay-up	Source	$\bar{w}_1$	$\bar{w}_2$	$\bar{w}_3$
SSSS	(0/90/90/0)	Present	10.5827	22.3750	26.2464
		Zamani et al. [26]	10.8137	22.7508	26.2021
	(30/60/60/30)	Present	11.3023	19.1494	27.7253
		Zamani et al. [26]	11.7158	19.1542	26.3149
CFSF	(0/90/90/0)	Present	7.0066	13.4300	16.9591
		Zamani et al. [26]	7.2436	13.5562	17.5084
	(30/60/60/30)	Present	4.4213	10.2217	13.8375
		Zamani et al. [26]	4.4120	10.1717	13.3471
CFFF	(0/90/90/0)	Present	1.9671	3.9469	8.7758
		Zamani et al. [26]	1.9660	3.9440	8.7862
	(30/60/60/30)	Present	0.8209	3.1551	5.3198
		Zamani et al. [26]	0.5721	3.3197	5.2285

Table 7
Static bending deflection and frequencies of free vibration for rhomboidal laminated plate with $a = 1$ and $b = 2$, $\left(\bar{w}|_A = w_0|_A \frac{E_2 h^3}{a^4 q_0} 100, \bar{\omega} = \frac{\omega a^2}{h}\sqrt{\frac{\rho}{E_2}}\right)$.

h/a	Lay-up	$\overline{W}\|_A$	$\bar{w}_1$	$\bar{w}_2$	$\bar{w}_3$
Point supported (four corners)					
0.05	(0/30/0)	11.9638	1.7920	4.4359	5.3728
	(0/90/0)	11.9544	1.8335	4.4652	5.3657
0.10	(0/30/0)	13.8528	1.6995	4.0872	5.0250
	(0/90/0)	13.8433	1.7471	4.1303	5.0428
0.20	(0/30/0) 19.8095	1.4825	3.3042	4.1946	
	(0/90/0)	20.0840	1.5393	3.3638	4.2426
SS (ed. 3 and 4) and point supported (one corner)					
0.05	(0/30/0)	11.4435	1.8455	5.3839	5.6827
	(0/90/0)	11.3323	1.8802	5.4863	5.6823
0.10	(0/30/0)	12.9058	1.7342	5.0397	5.1377
	(0/90/0)	12.7356	1.7763	5.1551	5.1787
0.20	(0/30/0)	16.8646	1.5064	4.1850	4.2847
	(0/90/0)	16.6583	1.5606	4.2502	4.4579

together all the like terms from any two adjacent elements which correspond to common nodal and edge degrees of freedom along their interface. Bardell et al. [21,22] demonstrated that the purely internal modes from one element cannot affect the purely internal modes from any other element, and so these contributions to the global stiffness and mass matrices and the global load vector remain unaffected by the assembly process.

By using the Hamilton's principle, the following relation can be written:

$$[M^G]\{\ddot{c}_{ij}\} - [K^G]\left\{c_{ij}^G\right\} + \{F^G\} = 0 \tag{23}$$

where $\{c_{ij}^G\} = \{c_{ij}^w, c_{ij}^{\phi x}, c_{ij}^{\phi y}\}$ is the unknown coefficients vector.

This is the basic governing equation to be solved for a general dynamic problem. For the special cases of static and free vibration problems this takes the familiar forms, respectively:

$$[K^G]\left\{c_{ij}^G\right\} = \{F^G\} \tag{24}$$

and

$$[M^G]\{\ddot{c}_{ij}^G\} - [K^G]\left\{c_{ij}^G\right\} = 0 \tag{25}$$

which leads to the following standard matrix-eigenvalue problem

$$([K^G] - \omega^2[M^G])\left\{c_{ij}^G\right\} = 0 \tag{26}$$

A variety of different boundary conditions may be applied to the plate, simply by removing from the stiffness matrix (and from the external forces vector or mass matrix) those rows and columns which correspond to the degrees of freedom $\left\{c_{ij}^G\right\}$ associated with an edge being simply supported, clamped or free, or a corner being point supported.

4. Verification and numerical results

4.1. Generalities

A computer code, based on the method developed in this paper, has been implemented and used for the analysis of plates having different shapes, material properties and boundary conditions. The presented results correspond to the dynamic and static analysis of the above mentioned plates. For the dynamic analysis, natural frequencies parameter and modal shapes were computed. While, for the static analysis, deflections were calculated under uniformly distributed loads. Although, in the present study, only plates under uniformly distributed loads are presented, the developed algorithm can handle many others applied loads.

In order to establish the accuracy and applicability of the described approach, numerical results were computed for a number of plate problems for which comparison values were available in the literature. Additionally, a number of new problems were solved. Calculations have been performed taking plates with different geometrical shapes, material properties, angles of fibre orientation, stacking sequences and a/h ratios.

Let us introduce the terminology to be used throughout the remainder of the paper for describing the boundary conditions of the plates considered. The designation CSFS, for example, identifies a plate with edges (1) clamped, (2) simply supported, (3) free and (4) simply supported (see Fig. 3). The subscripts 1 and 2 represent the directions parallel with and perpendicular to the fibre direction.

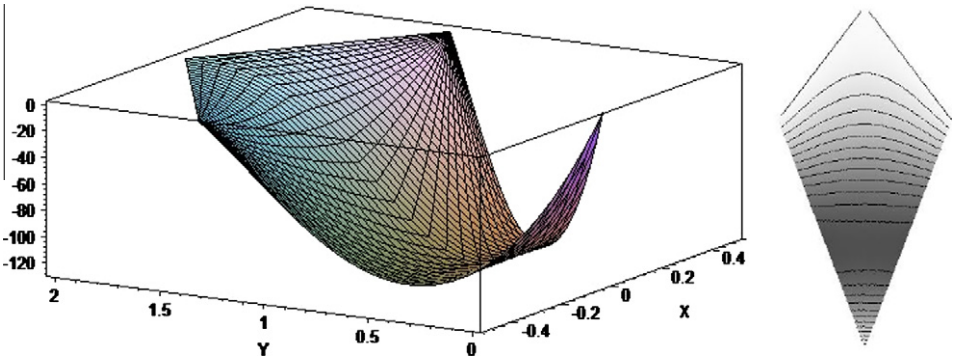

Fig. 4. Static bending deflections of (0/30/0) rhomboidal plate with $b = 2a$ and $h/a = 0.05$, obtained with the present method.

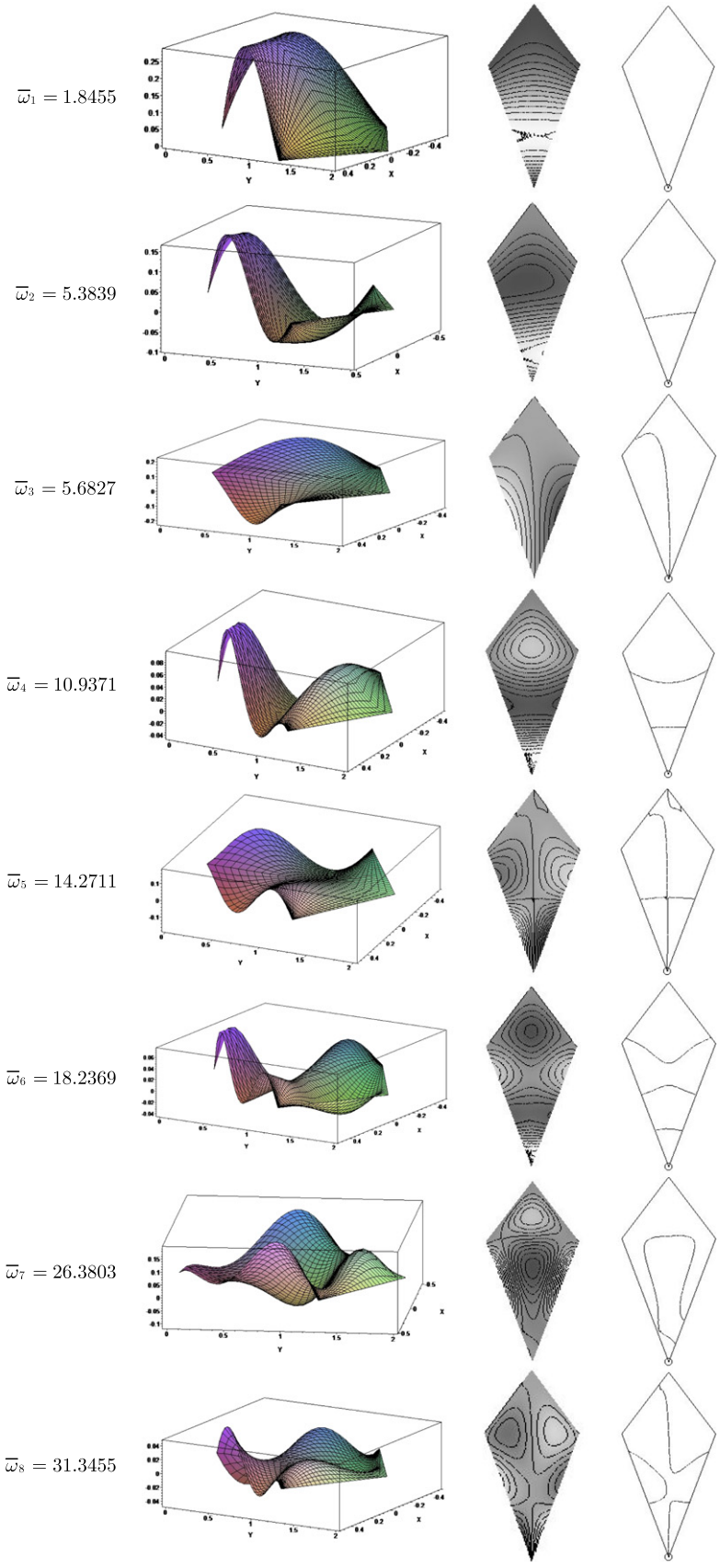

Fig. 5. Modal shapes and nodal patterns of (0/30/0) rhomboidal plate with $b = 2a$ and $h/a = 0.05$, obtained with the present method.

4.2. Convergence and comparison of static transverse deflections

The material properties for the layers of all laminates of Section 4.2 are $E_1 = 25E_2$, $G_{12} = G_{13} = 0.5E_2$, $G_{23} = 0.2E_2$, $\nu_{12} = 0.25$ and the shear correction factor is $k_s = 5/6$. In all cases the dimensionless deflection is given by $\overline{w} = 100w_0E_2h^3/(a^4q_0)$.

Results of a convergence study of central transverse deflections are presented in Table 1. This example considers a SFSF square laminated composite plate (Fig. 3a with $\theta_1 = \theta_2 = 0$ and $a = b$) under a uniformly distributed load of intensity q_0. The stacking sequence adopted is (90/0/90/0/90).

The convergence of the mentioned deflections is studied by gradually increasing the number of Gram–Schmidt polynomials used in each natural co-ordinate. It can be seen that $m, n = 4$, is sufficient to reach stable convergence. Results of Moleiro et al. [4] are presented alongside the numerical results for comparison purposes, showing an excellent agreement.

The accuracy and reliability of the deflections obtained with the presented method are also demonstrated in the following two cases. First, the centroidal deflection of a SSSS square laminated composite plate ($a = b$) is depicted in Table 2 and it is compared to those of Reddy [1], Belinha and Dinis [23] and Xiao et al. [24]. The second example considers a SSSS skew plate as shown in Fig. 3b. The centroidal deflection for a plate with $\alpha = 30°$ and $a = b = 1$ is tabulated in Table 3. The results are compared to those of Chakrabarti and Sheikh [25], and very good agreement is obtained. In both cases plates are subjected to a uniformly distributed load q_0, and the stacking sequence adopted is (0/90/0).

4.3. Convergence and comparison of natural frequencies

Results of a convergence study of dimensionless frequencies $\overline{\omega} = \frac{\omega b^2}{h}\sqrt{\frac{\rho}{E_2}}$ are presented in Table 4. This table shows the first three dimensionless natural frequencies of a moderately thick SFSF right trapezoidal plate (Fig. 3a), with $\theta_1 = 0$ and $\theta_2 = 45°$, and two different lay-up configurations. Composite material properties used in this study are: $E_1 = 40E_2$, $G_{12} = G_{13} = G_{23} = 0.6E_2$, $\nu_{12} = 0.25$, $\rho = 2500\ \text{kg/m}^3$, and the shear correction factor is $k_s = 5/6$. Results of Zamani et al. [26] are also included in Table 4 for comparison purposes. It can be concluded that predictions of the present method are in good agreement with the results of GDQ method presented by Zamani et al. [26]. Furthermore, results show that as the number of Gram–Schmidt polynomials increased results are rapidly converged to the final values which shows a fast rate of convergence of the method.

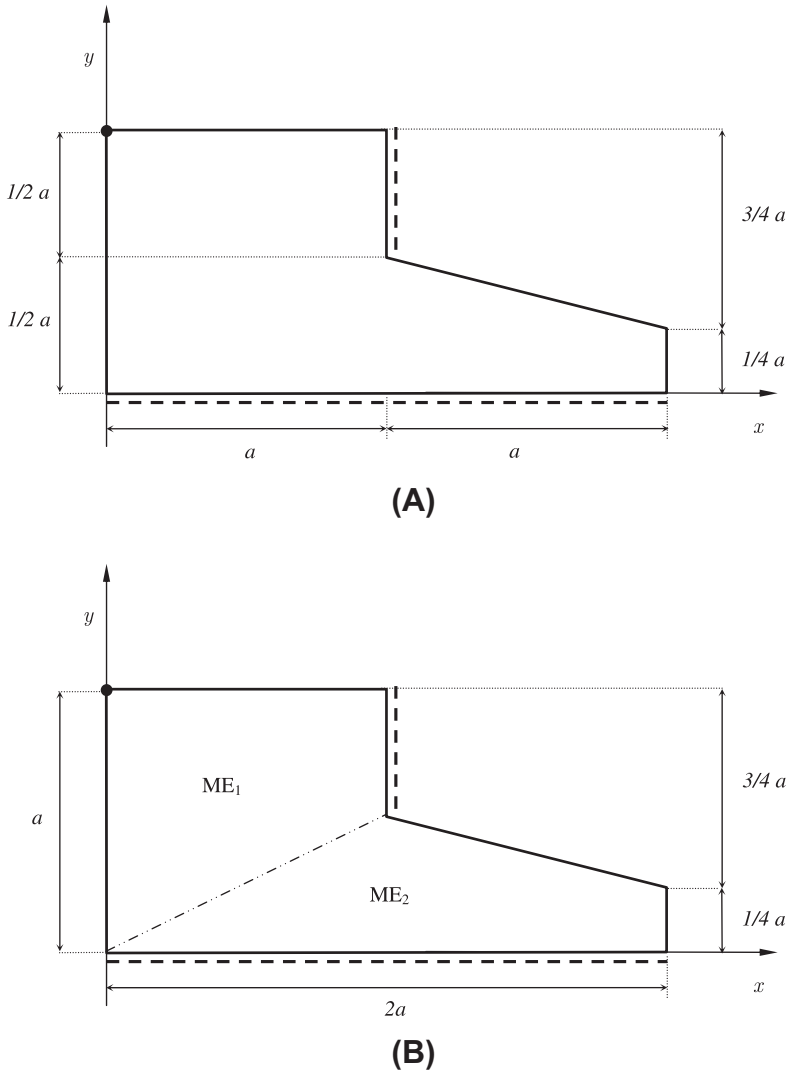

Fig. 6. Geometry of a L-planform laminated plate.

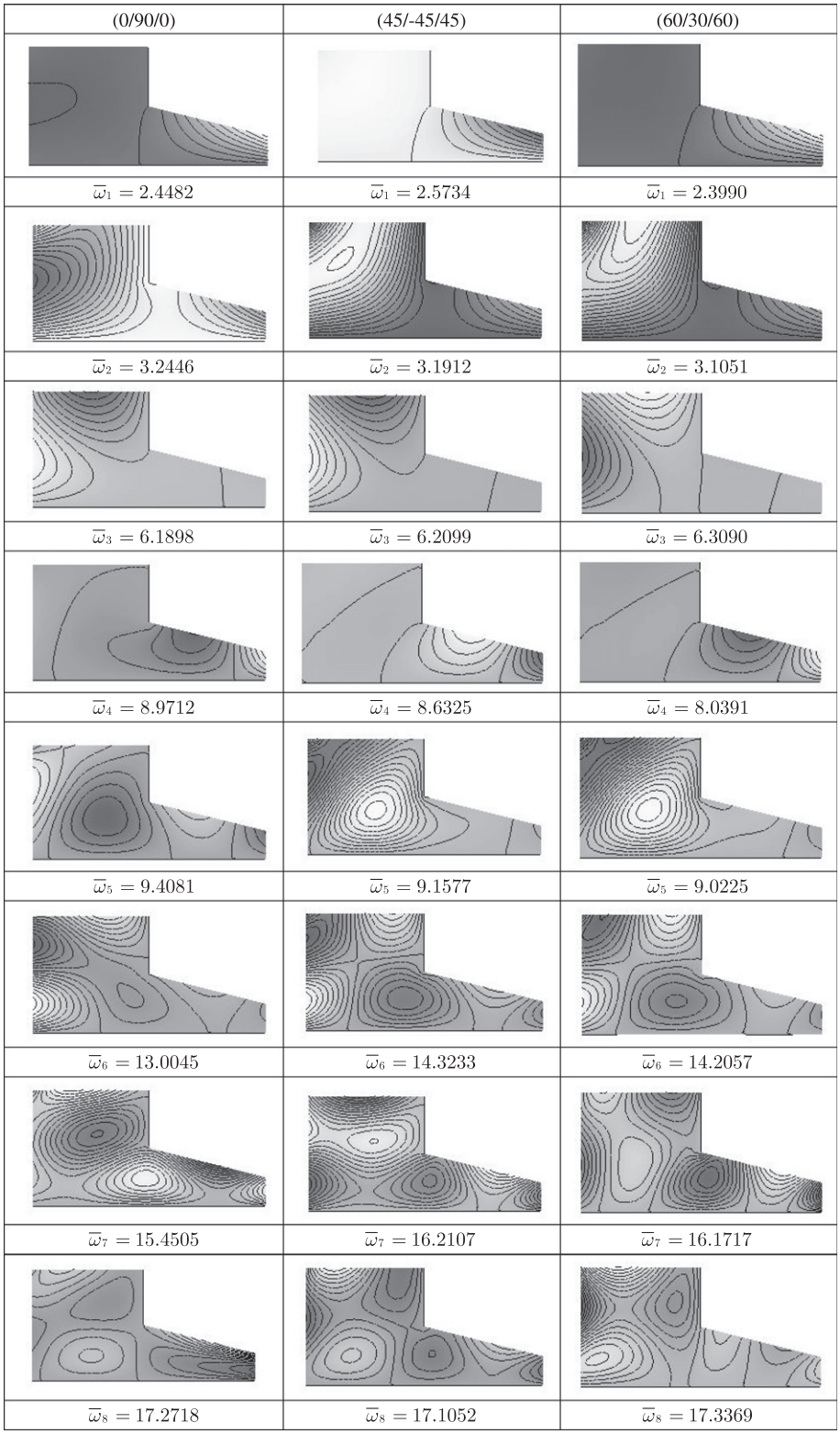

Fig. 7. Frequencies and nodal patterns of L-planform laminated plates with mixed boundary conditions.

In Table 5, frequency parameters $\bar{\omega} = \frac{\omega b^2}{\pi^2}\sqrt{\frac{\rho h}{D_0}}$ ($D_0 = \frac{E_2 h^3}{12(1-\nu_{12}\nu_{21})}$), for (0/90/0) square laminated plates, with SSSS and CCCC boundary conditions, and for various thickness ratios, are tabulated. In this case the material properties are $E_1 = 40E_2$, $G_{12} = G_{13} = 0.6E_2$, $G_{23} = 0.5E_2$, $\nu_{12} = 0.25$, and the shear correction factor is $k_s = \pi^2/12$. Results of Ferreira and Fasshauer [27] are also included for comparison purposes. From the results one can conclude that the present method leads to accurate results even using a few polynomials ($m,n = 4$).

Table 6 shows the first three dimensionless natural frequencies of the same right trapezoidal laminated plate (Fig. 3a) used for the

convergence study in Table 4. Again, present results are in good agreement with those of Zamani et al. [26].

4.4. Applications to rhomboidal plates

In this section, results are presented of the developed method applied to study the static and dynamic behaviour of rhomboidal laminates as shown in Fig. 3c. Three–ply E-glass/epoxy laminates ($E_1 = 60.7$ GPa, $E_2 = 24.8$ GPa, $G_{12} = 12$ GPa, $\nu_{12} = 0.23$), with stacking sequence $(0,\beta,0)$ are considered. As shown in Table 7 two different combinations of boundary conditions and various h/a ratios are taking into account.

For the static analysis, deflections in a specific point of the rhomboidal plate (point marked by A in Fig. 3c), under uniform distributed load q_0 are computed. For the dynamic analysis, the first three natural frequencies of free vibrations are determined.

As example, Figs. 4 and 5 present the static deflections and the modal shapes and nodal patterns of (0/30/0) rhomboidal plate with $b = 2a$ and $a/h = 0.05$, obtained with the present method, corresponded to a plate with edges (3) and (4) (see Fig. 3c) simply supported and a point supported at a corner defined by the intersection of edges (1) and (2).

4.5. Example of assembly of presented macroelements

Vibration analysis for a partially simply supported L-planform plate with a corner point supported at $x = 0$, $y = a$ (see Fig. 6a), is presented in this section. The plate structure was modelled using two macro-elements: ME_1 and ME_2 as shown in Fig. 6b. For this structure the first eight natural frequencies $\left(\bar{\omega} = \frac{\omega a^2}{h}\sqrt{\frac{\rho}{E_2}}\right)$ and modal shapes are depicted in Fig. 7, corresponding to a three-ply E-glass/epoxy laminates ($E_1 = 60.7$ GPa, $E_2 = 24.8$ GPa, $G_{12} = 12$ GPa, $\nu_{12} = 0.23$), with $h/a = 0.1$. In order to demonstrate the versatility of the presented formulation the free vibration characteristics frequency for three different stacking sequences are presented.

5. Conclusions

This article presents the formulation of an enriched plate element based on FSDT. This quadrilateral four-node laminated plate finite element has been formulated and generalized for being applied to anisotropic plates, with symmetric lamination scheme, and it is tested through the static and dynamic analysis in some numerical examples, producing very good results. It is possible to achieve very good accuracy in the results using a low number of polynomials and without densify the mesh in plates with general quadrilateral planform, which can be divided into a small number of macro-elements. The assembly example provides evidence of the versatility and capability of the current method.

Acknowledgements

The present investigation has been sponsored by the CONICET Project PIP 0105/2010, CIUNSA Project 1903 and REDES V Project, supported by SPU.

References

[1] Reddy JN. Mechanics of laminated composite plates and shells: theory and analysis. 2nd ed. Boca Raton, USA: CRC Press; 2003.
[2] Lekhnitskii SG. Anisotropic plates. New York: Gordon and Breach Science Publishers; 1968.
[3] Whitney JM. Structural analysis of laminated anisotropic plates. Pennsylvania, USA: Technomic Publishing Co. Inc.; 1987.
[4] Moleiro F, Mota Soares CM, Mota Soares CA, Reddy JN. Mixed least-squares finite element model for the static analysis of laminated composite plates. Comput Struct 2008;86:826–38.
[5] Auricchio F, Sacco E, Vairo G. A mixed FSDT finite element for monoclinic laminated plates. Comput Struct 2006;84:624–39.
[6] Wang J, Liew KM, Tan MJ, Rajendran S. Analysis of rectangular laminated composite plates via FSDT meshless method. Int J Mech Sci 2002;44:1275–93.
[7] Fares ME, Elmarghany MKh. A refined zigzag nonlinear first-order shear deformation theory of composite laminated plates. Compos Struct 2008;82:71–83.
[8] Xiang S, Wang K, Ai Y, Sha Y, Shi H. Analysis of isotropic, sandwich and laminated plates by a meshless method and various shear deformation theories. Compos Struct 2009;91:31–7.
[9] Ferreira AJM, Castro LMS, Bertoluzza S. A high order collocation method for the static and vibration analysis of composite plates using a first-order theory. Compos Struct 2009;89:424–32.
[10] Reissner E. The effect of transverse shear deformation on the bending of elastic plate. Am Soc Mech Eng J Appl Mech 1945;12:69–76.
[11] Mindlin RD. Influence rotatory inertia and shear in flexural motion of isotropic, elastic plates. ASME J Appl Mech 1951;18:31–8.
[12] Nallim LG, Oller S, Grossi RO. Statical and dynamical behaviour of thin fibre reinforced composite laminates with different shapes. Comput Methods Appl Mech Eng 2005;194:1797–822.
[13] Nallim LG, Oller S. An analytical–numerical approach to simulate the dynamic behaviour of arbitrarily laminated composite plates. Compos Struct 2008;85:311–25.
[14] Zienkiewicz OC, Taylor RL. The finite element method for solid and structural mechanics, 6th ed., vol. 2. Great Britain: Elsevier; 2005.
[15] Reddy JN. Finite element method. 2nd ed. New York: McGraw-Hill; 1993.
[16] Nallim LG, Grossi RO. On the use of orthogonal polynomials in the study of anisotropic plates. J Sound Vib 2003;264:1201–7.
[17] Rango RF, Nallim LG, Oller S. Formulation and assembly of hierarchical finite elements to the static and dynamic analysis of laminated quadrilateral plates. Rev Sul – Am Eng Estrut 2012;9:4–21.
[18] Bhat RB. Plate deflection using orthogonal polynomials. J Eng Mech 1985;111:1301–9.
[19] Bhat RB. Natural frequencies of rectangular plates using characteristic orthogonal polynomials in Rayleigh–Ritz method. J Sound Vib 1985;102:493–9.
[20] Bardell NS, Dunsdon JM, Langley RS. Free vibration analysis of thin rectangular laminated plate assemblies using the h-p version of the finite element method. Compos Struct 1995;32:237–46.
[21] Bardell NS, Dunsdon JM, Langley RS. Free vibration analysis of thin coplanar rectangular plate assemblies – Part I: Theory and initial results for specially orthotropic plates. Compos Struct 1996;34:129–43.
[22] Bardell NS, Dunsdon JM, Langley RS. Free vibration analysis of thin coplanar rectangular plate assemblies – Part II: Further results for generally orthotropic plates. Compos Struct 1996;34:145–62.
[23] Belinha J, Dinis LMJS. Analysis of plates and laminates using the element-free Galerkin method. Comput Struct 2006;84:1547–59.
[24] Xiao JR, Gilhooley DF, Batra RC, Gillespie Jr, McCarthy MA. Analysis of thick composite laminates using a higher-order shear and normal deformable plate theory (HOSNDPT) and a meshless method. Composites: Part B 2008;39:414–27.
[25] Chakrabarti A, Sheikh AH. A new triangular element to model inter-laminar shear stress continuous plate theory. Int J Numer Methods Eng 2004;60:1237–57.
[26] Zamani M, Fallah A, Aghdam MM. Free vibration analysis of moderately thick trapezoidal symmetrically laminated plates with various combinations of boundary conditions. Eur J Mech A/Solids 2012;36:204–12.
[27] Ferreira AJM, Fasshauer GE. Analysis of natural frequencies of composite plates by an RBF-pseudospectral method. Compos Struct 2007;79:202–10.